Journal of Biomedical Optics

SPIEDigitalLibrary.org/jbo

Ray-tracing optical modeling of negative dysphotopsia

Xin Hong
Yueai Liu
Mutlu Karakelle
Samuel Masket
Nicole R. Fram

SPIE

Ray-tracing optical modeling of negative dysphotopsia

Xin Hong,[a] Yueai Liu,[a] Mutlu Karakelle,[a] Samuel Masket,[b] and Nicole R. Fram[b]
[a] Alcon Laboratories, 6201 South Freeway, Fort Worth, Texas 76134
[b] Jules Stein Eye Institute, UCLA Center for Health Sciences, 100 Stein Plaza, Los Angeles, California 90095

Abstract. Negative dysphotopsia is a relatively common photic phenomenon that may occur after implantation of an intraocular lens. The etiology of negative dysphotopsia is not fully understood. In this investigation, optical modeling was developed using nonsequential-component Zemax ray-tracing technology to simulate photic phenomena experienced by the human eye. The simulation investigated the effects of pupil size, capsulorrhexis size, and bag diffusiveness. Results demonstrated the optical basis of negative dysphotopsia. We found that photic structures were mainly influenced by critical factors such as the capsulorrhexis size and the optical diffusiveness of the capsular bag. The simulations suggested the hypothesis that the anterior capsulorrhexis interacting with intraocular lens could induce negative dysphotopsia. [DOI: 10.1117/1.3656745]

Keywords: capsulorrhexis; cataract extraction; human eye; intraocular lens; optical simulation; optical diffusiveness; photonic phenomena; pupil size; Zemax ray-tracing technology..

Paper 11251R received May 19, 2011; revised manuscript received Sep. 13, 2011; accepted for publication Oct. 5, 2011; published online Nov. 22, 2011.

1 Introduction

Optical side effects are well-documented associated symptoms of visually undesired photic phenomena following an intraocular lens (IOL) implantation surgery. The manifestations of the photic phenomena include transient glare, streaks, arcs, halos, and edge effects and have been collectively described as dysphotopsia. The term dysphotopsia was originally introduced by Tester and co-workers in 2000.[1] The photic phenomena can occur either as a positive or negative dysphotopsia. Positive dysphotopsia is perceived by patients as brightness, halos, or streaks, and rays emanating from a central point source of light, sometimes with a diffuse hazy glare. Conversely, negative dysphotopsia is characterized by the perception of dark shadows of crescent shape, which can be arc-shaped, usually in the temporal field of vision.[2–4]

The prevalence of dysphotopsia after cataract surgery and IOL implantation is unknown and its incidence varies widely. In a study by Shambu and co-workers[5] involving 111 patients who underwent uncomplicated cataract surgery, the reported overall incidence of dysphotopsia was 77.7%. Tester et al.[1] reported that 49% of the 302 patients had some type of dysphotopsia after cataract extraction with implantation of IOL. In another study, Bournas et al.[6] demonstrated that 117 (19.5%) of the 600 patients reported dysphotopsia during the first follow-up visit. Conversely, Davison et al.[2] showed that only 0.2% (14 of 6,668 cases) of patients reported dysphotopsia after cataract extraction with IOL implantation. This study further determined that 6 of the 14 patients had positive dysphotopsia, 6 negative dysphotopsia, and 2 combined features.

Negative dysphotopsia is a relatively common complication and poorly understood photic phenomenon that may follow cataract surgery with in-the-bag implantation of a posterior chamber IOL.[2–4] The physiological mechanisms leading to negative dysphotopsia remain an enigma, and its causative factors have been elusive. However, negative dysphotopsia has been described as the most troublesome complaint after uneventful IOL implantation surgery.[3,7] Although this visual phenomenon is tolerable by most patients and its magnitude usually lessens or disappears over time, it becomes a bothersome symptom for some patients, and may even result in secondary surgery in the worst cases. Many experts believe that the edge of the IOL causes the patient to perceive a temporal shadow and have noted this with a wide variety of IOL designs.[2–4,7] Other proposed causes of negative dysphotopsia include individual predisposition, optical interference of light, and complex interactions between the IOL optics and the optics of the eye.

Optical modeling or simulation plays a central role in deriving new experimental knowledge to better understand the precise biological system and optical design of the eye. In the present investigation, we attempted to establish an optical model to simulate the photic phenomenon experienced by the human eye on the peripheral retina. Findings from the optical modeling support the hypothesis originally proposed by Masket and Fram[8] that the negative dysphotopsia may be considered a complication of anterior capsulorrhexis with in-the-bag IOL implantation.

2 Methods

2.1 *Zemax Optical Modeling*

Negative dysphotopsia was studied with nonsequential-component (NSC) Zemax (Radiant Zemax, Bellevue, Washington) ray-tracing of a model pseudophakic eye based on a mid-power Alcon AcrySof® IQ lens (20D SN60WF), as shown in Fig. 1. The solid models of the IOL optics and haptics were generated with pro-E (Parametric Technology Corporation, Needham, Massachusetts) software and then imported to Zemax. The anterior capsular bag was assumed to conform to the anterior IOL surface and the posterior capsular bag to the posterior

Address all correspondence to: Xin Hong, Alcon Laboratories, Inc., Surgical Optics Research, 6201 South Freeway, Fort Worth, Texas 76134; Tel: 817-615-2589; Fax: 817-615-3894; E-mail: xin.hong@alconlabs.com.

1083-3668/2011/16(12)/125001/7/$25.00 © 2011 SPIE

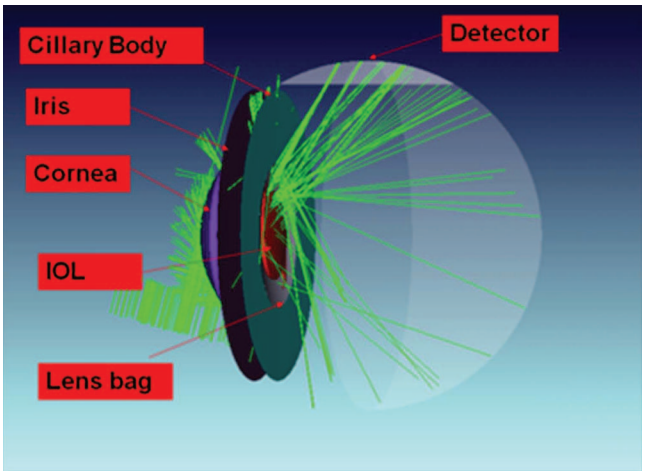

Fig. 1 Schematic drawing of the NSC modeling in Zemax to show the major optical components and the light passages after reflected and refracted by the components.

IOL surface. The ciliary processes may have blocked some part of the direct light sneaking through the gap between the IOL optics and the iris; however, modeling with and without ciliary processes revealed no or little noticeable differences.

The detector was part of a sphere with a 6 mm aperture contoured as the retinal shape and centered on the primary image formed by temporal incident light 75° off-axis from optical infinity. Virtual Zemax detectors are used in the simulation to detect distribution of light intensity at desired locations on the retina surface. The virtual detector used in the simulation was shaped as part of a sphere with a 6 mm aperture contoured as the retinal shape and centered on the primary image location formed by temporal incident light 75° off-axis from optical infinity. Like the retina that responds to illumination, the detector typically detects the light intensity on a linear scale. However, the logarithmic scale was used to examine the optical details of the photics. The final image on the detector consisted of a primary image formed through the optic, multiple reflections formed by surfaces, edges and haptics, and direct light that missed the IOL body totally.

The causal relationship between optical features and photic structures was examined by focusing on individual components (e.g., surfaces, edges, or haptics) while blocking all other components using ray-tracing technology.

2.2 *Modeling Parameters and Conditions*

This parametric modeling included variables such as diffusiveness of the capsular bag, capsulorhexis size, and pupillary diameter. The opacification of the lens capsule is caused by a layer of granulated calcium deposition. The optical property of this opacification is diffusive. When a beam of light strikes onto the deposition, it is scattered around in all directions. The nature of the scattering can be characterized by Lambertian scattering. We hypothesized that the anterior capsular bag would initially be clear (100% transparent) and eventually would become somewhat opaque, which could be modeled as a Lambertian diffusive component. For Lambertian scattering, the scattered ray-projection vector has equal probability anywhere in the unit circle, and the bi-directional scatter distribution function is just $1/\pi$. The scattered intensity is proportional to $\cos\theta$, where θ is

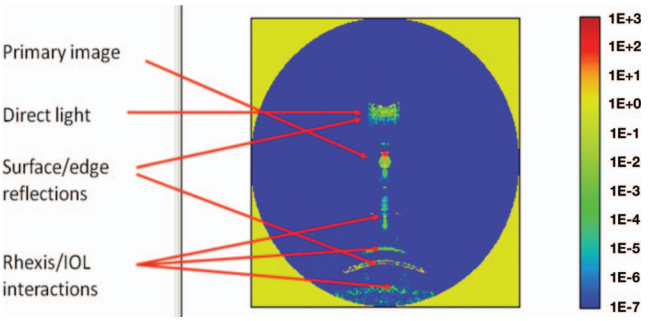

Fig. 2 The primary image, surface/rhexis reflections, and direct lights on the retinal detector were graphically illustrated in logarithmic intensity plot.

the angle of observation. This is worth emphasizing that Lambertian scattering is independent on the ray-incident angle, and most diffuse surfaces are nearly Lambertian.

The capsulorrhexis size was designated as 3 and 6 mm, as two extremes in practice. The capsulorrhexis opening was assumed to be circular. Two pupil sizes were evaluated: a 3-mm pupil for the photopic condition and a 6-mm pupil for the scotopic condition.

To obtain reliable optical predictions, 100,000 rays were traced through the optical system for each computation. The options of multiple reflections and scattering were turned on to allow the physical modeling of complex light passages in the multiple-component system before reaching the retina. The extensive ray-tracing slowed down the computational turnaround time; hence, the contribution of each optical component was verified to ensure calculation accuracy, as illustrated in Fig. 2.

3 Results

In this study, the NSC Zemax simulation illustrated that multiple reflections and direct lights generated photic structures at much lower intensities than the primary image [Fig. 3(a)]. That might help to explain why the negative dysphotopsia or photic phenomena were not common concerns for pseudophakic patients with monofocal implants and might manifest under certain lighting conditions such as extended light sources or bright ambient lights. It was also imperative that simulation images be examined with a logarithmic scale, as shown in Fig. 3(b), in order to relate to the human visual system for brightness perception and contrast recognition.[9–11] The low-intensity details, which were often hardly noticeable in the linear-intensity plot, could indicate the possibility of increased photic observation with appropriate lighting conditions.

With a clear capsule bag, a small capsulorrhexis (3 mm circular opening), and a small pupil (3 mm), photic structures formed by multiple reflections and direct light were clearly visible when examined with logarithmic scales, as shown in Fig. 3(b). Multiple gaps between the primary image, multiple reflections, and direct light were easily identified and could manifest themselves as a negative dysphotopsia clinically.

3.1 *Effects of Capsulorhexis Size and Bag Diffusiveness with a Small Pupil Size (3 mm)*

The small pupil condition (3 mm) was examined first, as shown in Fig. 4, primarily because most visual activities occur in

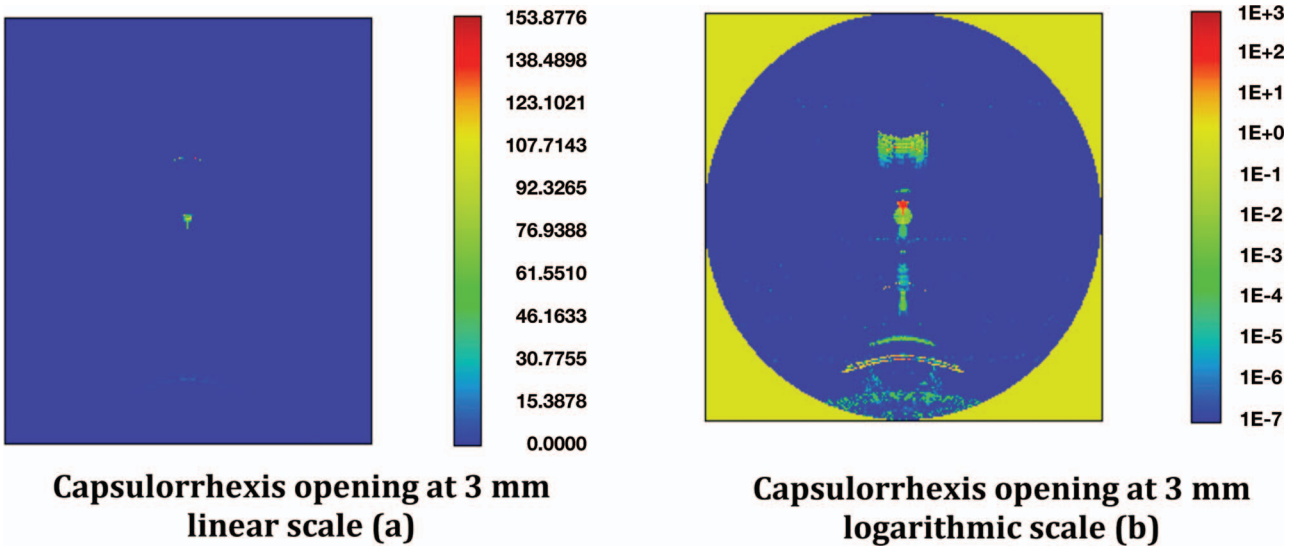

Fig. 3 The simulated retinal image for 20D SN60WF IOL with a 3 mm capsulorrhexis opening and a 3 mm pupil displayed in (a) linear scale and (b) logarithmic scale, respectively.

photopic conditions. Figure 4 shows the NSC Zemax simulated images of two rhexis opening sizes (3 and 6 mm) and two different diffusive levels of the capsular bag (clear and 50% diffusive). The diffusive capsular bag reduced the contrast among photic structures by creating a uniformly scattered light on the detector serving as the background of the image, as shown in Figs. 4(b) and 4(d). Especially, where the rhexis opening size was 3 mm, it could be a larger diffusive capsular bag remnant. Consequently,

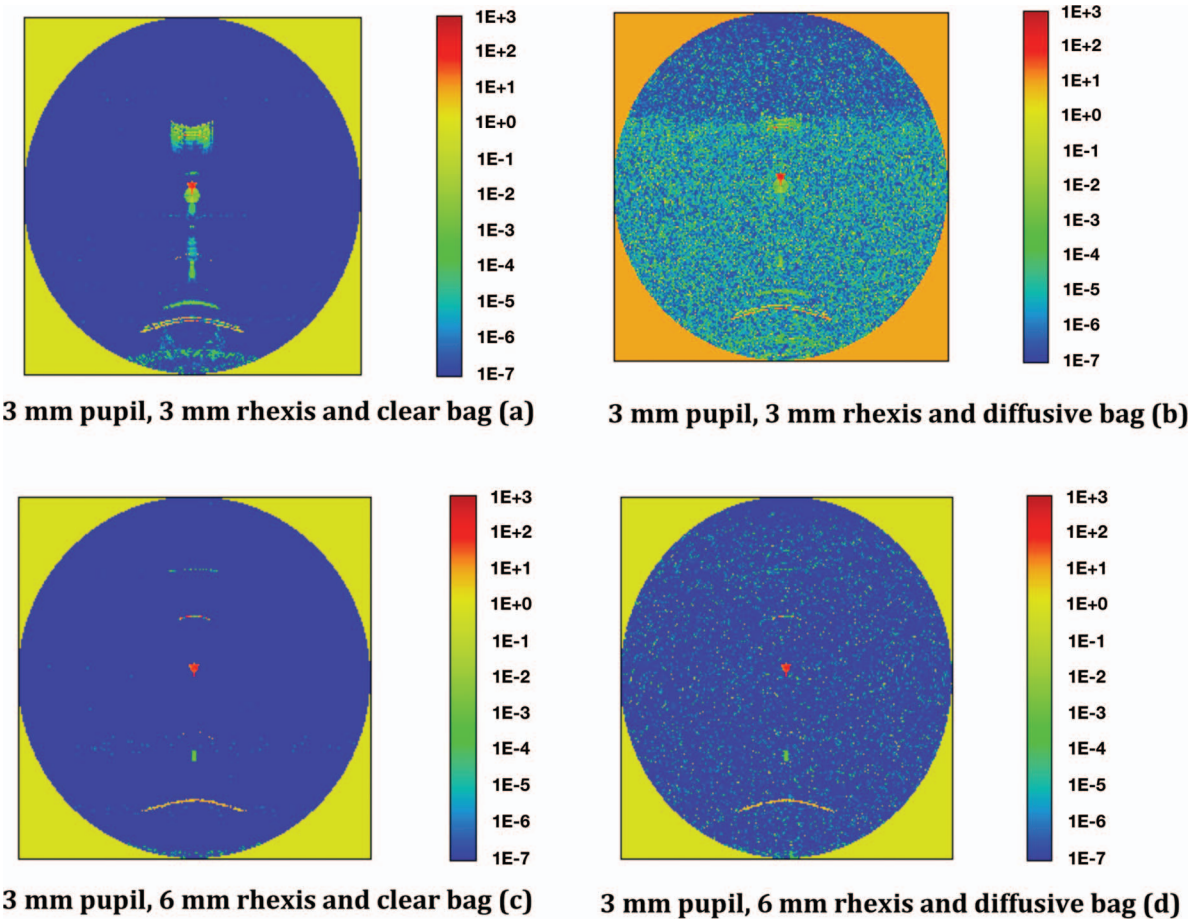

Fig. 4 The retinal images were simulated for a small pupil (3 mm) under the combined conditions of a small (3 mm)/large (6 mm) rhexis and clear/diffusive bags. (a) Retinal images simulated for 3 mm pupil/3 mm rhexis and clear bag. (b) Retinal images simulated for 3 mm pupil/3 mm rhexis and diffusive bag. (c) Retinal images simulated for 3 mm pupil/6 mm rhexis and clear bag. (d) Retinal images simulated for 3 mm pupil/6 mm rhexis and diffusive bag. All the plots are in logarithmic scales.

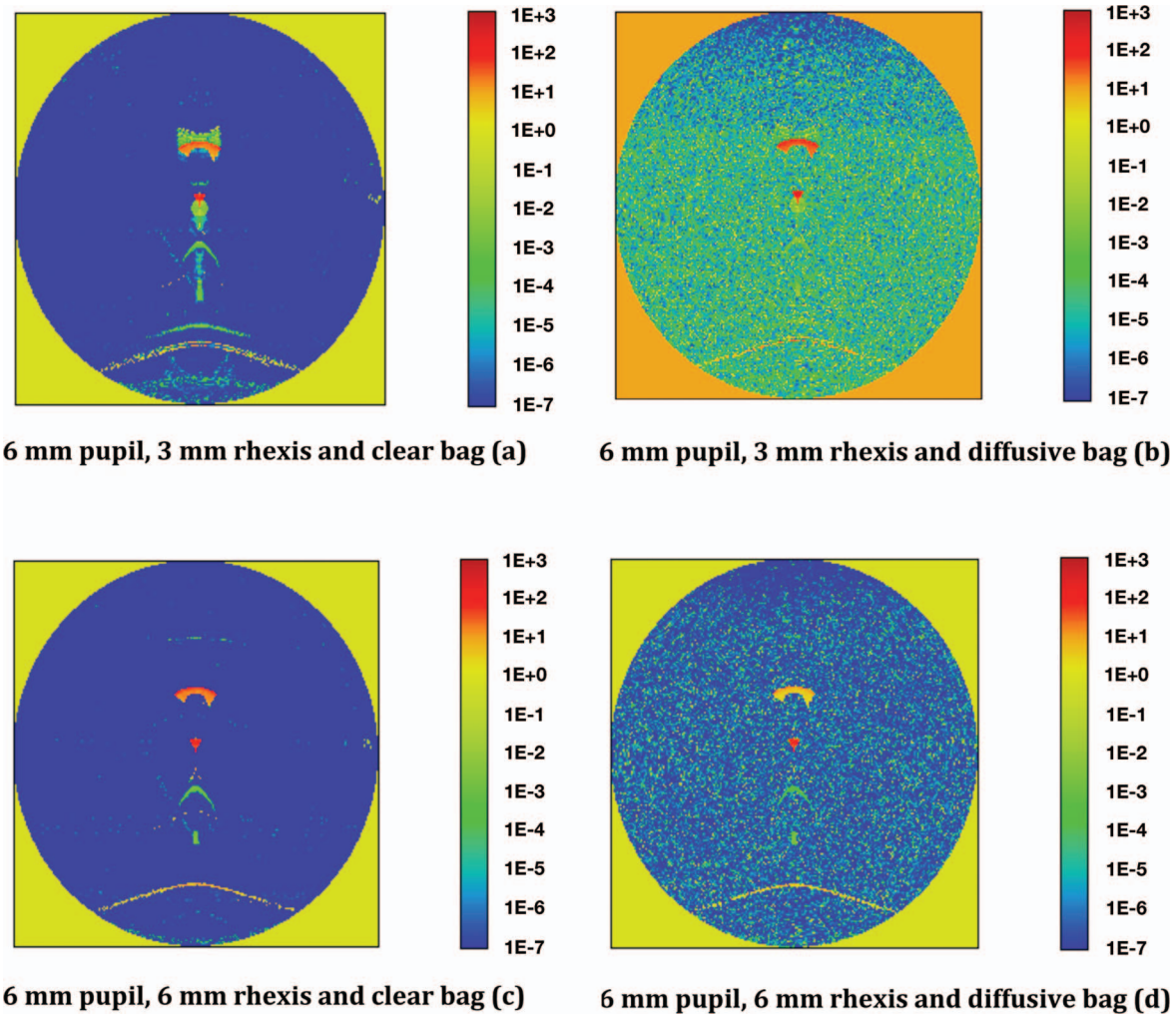

Fig. 5 The retinal images were simulated for a large pupil (6 mm) under the combined conditions of a small (3 mm)/large (6 mm) rhexis and clear/diffusive bags. (a) Retinal images simulated for 6 mm pupil/3 mm rhexis and clear bag. (b) Retinal images simulated for 6 mm pupil/3 mm rhexis and diffusive bag. (c) Retinal images simulated for 6 mm pupil/3 mm rhexis and clear bag. (d) Retinal images simulated for 6 mm pupil/3 mm rhexis and diffusive bag. All the plots are in logarithmic scales.

the intensity contrasts between primary images and photic structures (multiple reflections, and direct lights) were diminished [Fig. 4(b)]. This simulation result supported clinical observations that patients report negative dysphotopsia more often immediately after cataract surgery than at later timeframes, presumably due to increased fibrosis with loss of optical clarity.

Different from the effect of diffusive capsular bag, the large capsulorrhexis did not create rhexis-related structures on the retina, as shown by comparing observations with a small rhexis opening [3 mm; Fig. 4(a)] and a large rhexis opening [6 mm; Fig. 4(c)]. The capsular bag has a different refractive index than the IOL and aqueous humor; therefore, the light is refracted and reflected at the interfaces. The bag's interactions with the IOL and aqueous humor created several distinct structures, and the larger capsulorrhexis opening significantly reduced the photic structures. Combined with a diffusive bag, the large capsulorrhexis further minimized the possibility of photic phenomena, as shown in Fig. 4(d).

3.2 *Effects of Capsulorhexis Size and Bag Diffusiveness with a Large Pupil Size (6 mm)*

The simulation was repeated for a 6 mm pupil size (as in scotopic conditions) and the combined conditions of small (3 mm)/large (6 mm) rhexis and clear/diffusive bags. The findings upon optical simulation are shown in Fig. 5. The findings observed with the 6 mm pupil size reflect those observed with the 3 mm pupil size. However, one difference worth mentioning for the 6 mm pupil size was the increased intensity of direct light due to the increased space between the iris and the IOL optics.

3.3 *Impact of a Piggyback Intraocular Lens and Reverse-Optic-Capture on Photic Structures*

In order to further compare our findings with clinical observations, similar simulations were carried out for piggyback IOL and reverse-optic-capture (ROC) situations. The simulation results for the piggyback IOL are shown in Figs. 6 and 7. A plano

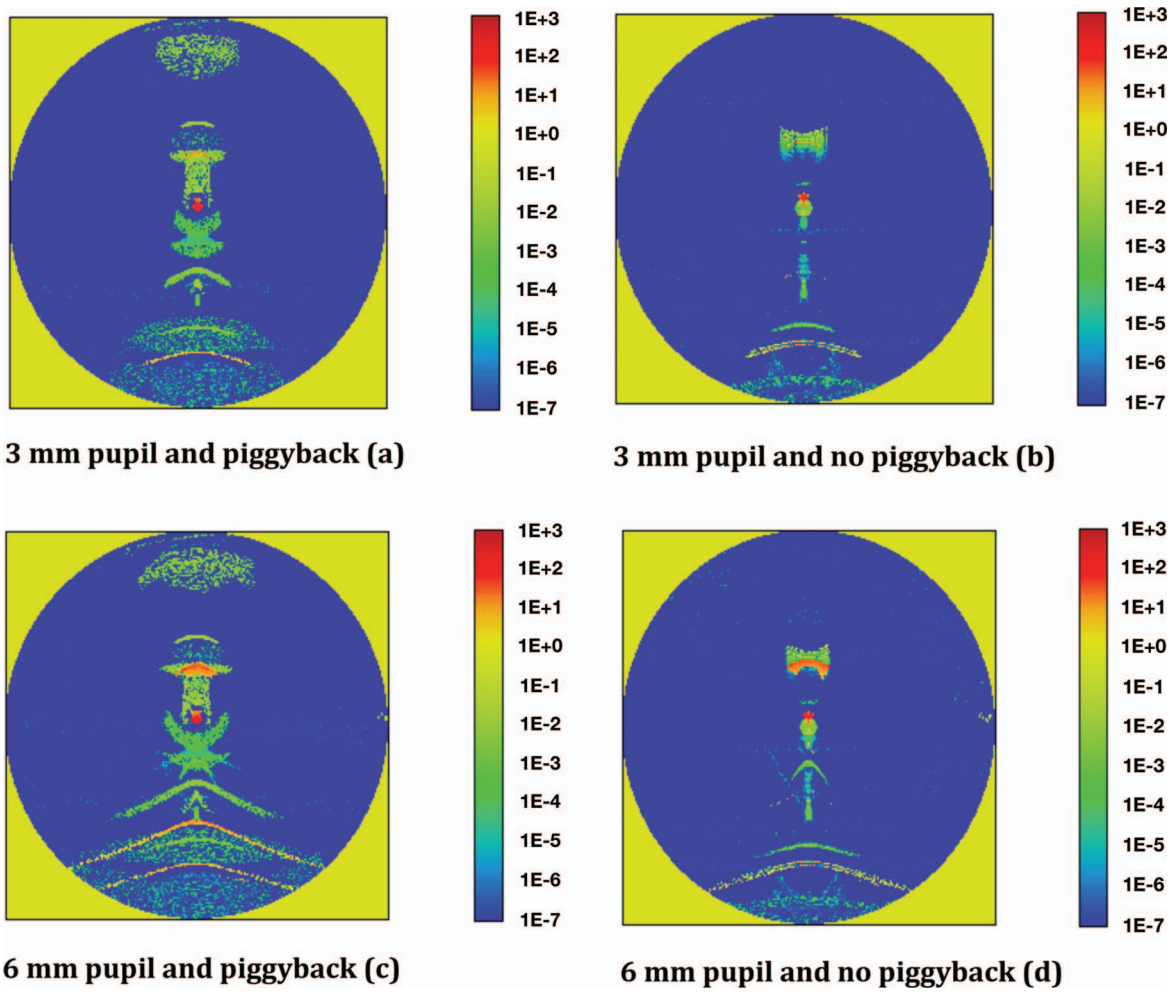

Fig. 6 The retinal images were simulated with and without piggyback IOL, for small (3 mm)/large (6 mm) pupils. (a) Retinal images simulated with piggyback for 3 mm pupil. (b) Retinal images simulated without piggyback for 3 mm pupil. (c) Retinal images simulated with piggyback for 6 mm pupil. (d) Retinal images simulated without piggyback for 6 mm pupil. All the plots are in logarithmic scales.

Table 1 Summary of clinical observations and hypothesis testing of proposed etiology of retinal projection of the interface between anterior capsulorrhexis and IOL surface.

Clinical findings (Masket)[a]	Hypothesis – rhexis-IOL interaction creates visible arcs/bands and intensity gaps between them could contribute to dark-arc sensation
Temporal dark crescent at 60 deg to 90 deg	Observable at 75 deg, to be conformed at <60 deg
"Horse blinders" describes and resolves symptoms	Eliminating peripheral lighting is expected to resolve this issue
Common early after surgery, but generally remits	Diffusive capsular bag caused by fibrosis may explain the remission
Stimulated by peripheral point light source	Simulated the point source at 75 deg
Symptoms worse when pupils constricted, better when dilated	Relatively invariant with pupils, not mitigated when dilated
Associated with ANY incision and ANY in-the-bag IOL	Independent of incision, IOL designs and materials
Only with "anatomically perfect surgery"	Perfect round rhexis is simulated; irregular rhexis not modeled
Symptoms may be unilateral despite similar anatomy	Not simulated; might be related to visual perception
Not reported with sulcus-placed PC IOLs or AC IOLs	Reduced intensity contrast between bright/dark bands/arcs
Not reported with reverse optic capture	Reduced number of bands/arcs

[a]References 12 and 13.

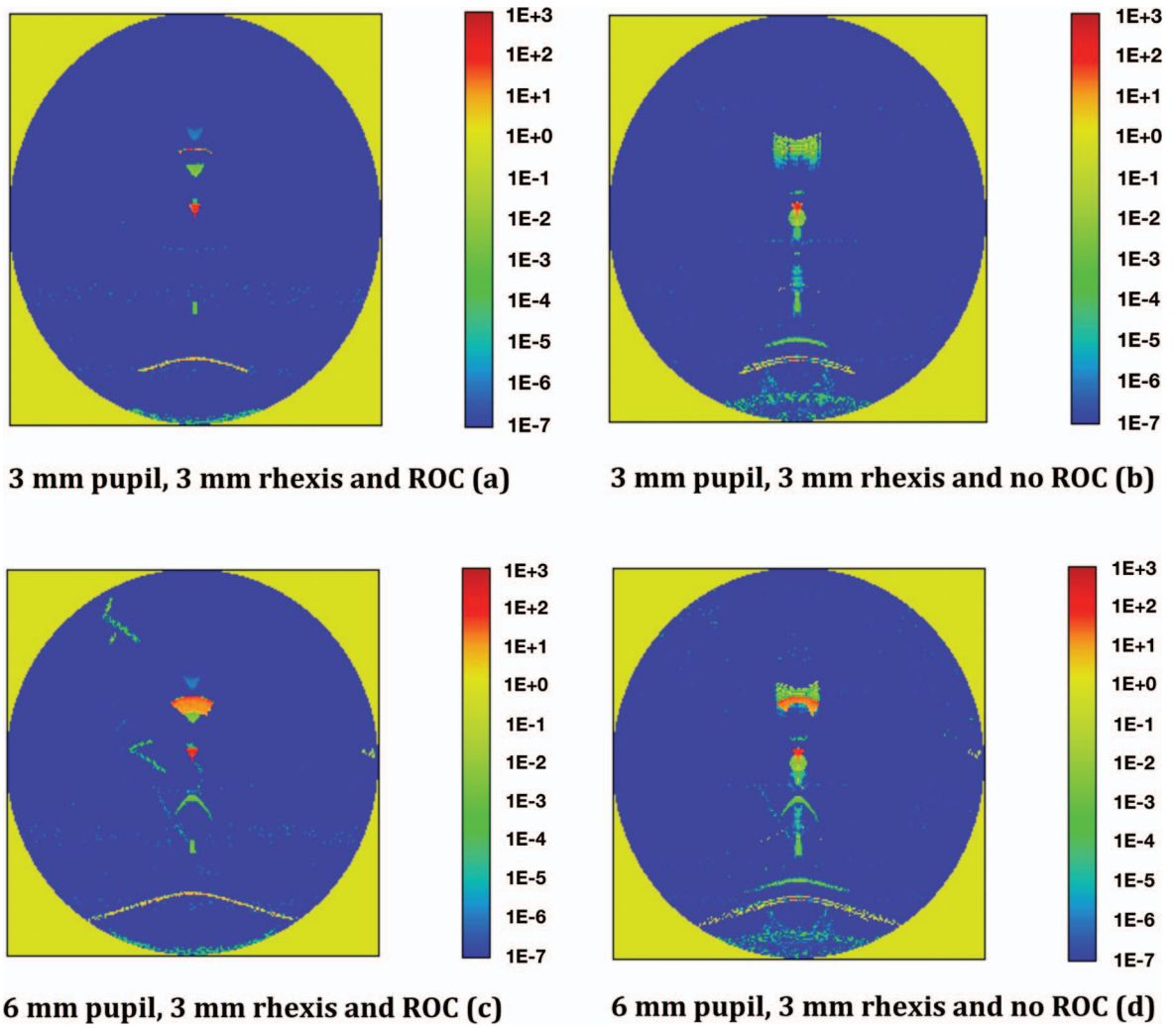

Fig. 7 The retinal images were simulated for reverse-optic-capture (ROC) condition for small (3 mm)/large (6 mm) pupils. (a) Retinal images simulated for 3 mm pupil/3 mm rhexis and ROC. (b) Retinal images simulated for 3mm pupil/3 mm rhexis and no ROC. (c) Retinal images simulated for 6 mm pupil/3 mm rhexis and ROC. (d) Retinal images simulated for 6 mm pupil/3 mm rhexis and no ROC. All the plots are in logarithmic scales.

piggyback IOL was intentionally placed in front of the monofocal IOL with direct vertex-to-vertex contact. The addition of a piggyback IOL into the optical system increased multiple reflections and ghost images. As a consequence, we observed more photic structures associated with multiple reflections by the piggyback IOL and its interactions with the other optical components [as shown in Figs. 6(a) and 6(c)]. However, the multiple reflections seemed to bridge the gaps between the structures formed by the in-bag IOL alone [as shown in Figs. 6(b) and 6(d)], hence, reduced the visibility of gap structures.

In the case of reverse-optic-capture, the anterior capsular bag was moved to the posterior side to mimic clinical practice, as depicted in Fig. 7. This relocation caused the shift of photic structures related to the anterior bag and hence may have reduced the contrast, the gap, or both.

4 Discussion

Ray-tracing simulation supported the optical basis for the clinical observation of negative dysphotopsia and found two critical impact factors: capsulorhexis size and optical diffusiveness of capsular bag. Both of these critical impact factors were related to the anterior capsular bag. The simulations thus supported the hypothesis that the anterior capsule remnant may induce negative dysphotopsia. The computations further suggested that the following approaches might mitigate the clinical risk of negative dysphotopsia:

- Reduce the visibility of photic structures on the retina with novel IOL designs specifically targeting negative dysphotopsia.
- Awaiting the natural process of anterior capsular opacification to occur and then diffuse the incoming light, which would result in less negative dysphotopsia.
- Trying either piggyback or reverse-optic-capture options to bridge or offset the intensity gaps and make the photic structures less distinguishable. In practice, piggyback and ROC approaches can be taken either pre-emptively or as second surgical intervention. Implementing such strategies requires the identification of likely patients or the secondary surgical intervention.

Based on the findings of this ray-tracing optical modeling, it is hypothesized that an interaction between capsulorrhexis and IOL may lead to negative dysphotopsia following IOL implantation. The hypothesis states that capsulorrhexis-IOL interaction may produce visible arcs and bands and the intensity gaps between visible arcs/bands could contribute to dark-arc sensation. The dark shadow perception would be further enhanced if an extended light source was present along the direction of visible arcs due to the integration of light energy along the same direction. Furthermore, the proposed hypothesis may help to explain major clinical observations, as summarized in Table 1.[12,13] The hypothesis further suggested that rhexis-IOL interaction could be the root cause of patient-reported negative dysphotopsia.

The simulation did not explicitly clarify all clinical observations related to negative dysphotopsia. For instance, the intensity levels associated with photic structures were much lower than with primary images, and the crescent-shaped dark shadow was not directly visualized. We believe that the lack of a clear crescent shape might be related to the lighting conditions, whether extended light sources or bright ambient lighting. The direct link between the deficiency of light intensity and dark-shadow sensation was not experimentally established. It is conceivable, however, from the scientific point-of-view that the deficiency of light intensity would be viewed as dark when compared to the surroundings. The dark strip will be formed when changing light source from the point source to an extended one. This is consistent with the clinical description of negative dysphotopsia as the patient-reported observation of a dark crescent in the temporal field.

Additionally, the image formed by direct light became more obvious with the larger pupil size, which was inconsistent with the clinical observation that the perception of dark shadow lessened with a large pupil. Perhaps this was because high-order aberrations of the off-axis human eye were not completely factored into the simulation. It is well known that the human eye has considerable off-axis high-order-aberrations at large pupil sizes. This may blur images and diminish gaps between primary image and images formed by direct light and multiple reflections.

Overall, the findings from the ray-tracing optical modeling/simulation support the optical basis of negative dysphotopsia. Thus, this study will provide an important insight for future investigation of negative dysphotopsia symptoms associated with implantation of IOLs.

Acknowledgments

The medical writing assistance for this manuscript was provided by G. Kesava Reddy, PhD, MHA, and the study was funded by Alcon Laboratories, Inc.

References

1. R. Tester, N. L. Pace, M. Samore, and R. J. Olson, "Dysphotopsia in phakic and pseudophakic patients: incidence and relation to intraocular lens type(2)," *J. Cataract Refract. Surg.* **26**(6), 810–816 (2000).
2. J. A. Davison, "Positive and negative dysphotopsia in patients with acrylic intraocular lenses," *J. Cataract Refract. Surg.* **26**(9), 1346–1355 (2000).
3. R. H. Osher, "Negative dysphotopsia: long-term study and possible explanation for transient symptoms," *J. Cataract Refract. Surg.* **34**(10), 1699–1707 (2008).
4. W. B. Trattler, J. C. Whitsett, and P. A. Simone, "Negative dysphotopsia after intraocular lens implantation irrespective of design and material," *J. Cataract Refract. Surg.* **31**(4), 841–845 (2005).
5. S. Shambhu, V. A. Shanmuganathan, and S. J. Charles, "The effect of lens design on dysphotopsia in different acrylic IOLs," *Eye (Lond)* **19**(5), 567–570 (2005).
6. P. Bournas, S. Drazinos, D. Kanellas, M. Arvanitis, and E. Vaikoussis, "Dysphotopsia after cataract surgery: comparison of four different intraocular lenses," *Ophthalmologica* **221**(6), 378–383 (2007).
7. P. Vamosi, B. Csakany, and J. Nemeth, "Intraocular lens exchange in patients with negative dysphotopsia symptoms," *J. Cataract Refract. Surg.* **36**(3), 418–424 (2010).
8. S. Masket and N. R. Fram, "Pseudophakic negative dysphotopsia: Surgical management and new theory of etiology," *J. Cataract Refract. Surg.* **37**(7), 1199–1207 (2011).
9. H. Gross, E. Blechinger, and B. Achtner, "Human Eye," in *Handbook of Optical Systems: Survey of Optical Instruments*, pp. 23–24, Wiley-VCH, Weinheim, Germany (2008).
10. R. F. Hess, "The Edridge-Green lecture vision at low light levels: role of spatial, temporal and contrast filters," *Ophthalmic Physiol. Opt.* **10**(4), 351–359 (1990).
11. F. L. Nes and M. A. Bouman, "Spatial modulation transfer in the human eye," *J. Opt. Soc. Am.* **57** 401–406 (1967).
12. S. Masket, "Ultrasound biomicroscopy for evaluation of negative dysphotopsia," presented at *American Society of Cataract and Refractive Surgery*, San Francisco (April 2009).
13. S. Masket, "Managing pseudophakic 'Dysphotopsia'," presented at *American Association of Ophthalmology*, San Francisco (October 2009).